

IN SILICO CHOLINERGIC ACTIVITY OF BIOACTIVE COMPOUNDS FROM CITRUS SINENSIS PEEL ON TYPE 2 DIABETES MELLITUS AND ALZHEIMER'S DISEASE

Ajiboye, B.O

Phytomedicine, Biochemical Toxicology and Biotechnology Research Laboratory
Department of Biochemistry, College of Sciences, Afe Babalola University, Ado-Ekiti

*bash1428@yahoo.co.uk or ajiboyebo@abuad.edu.ng

Abstract

The present study was aimed at assessing the *in silico* cholinergic activity of bioactive compounds from *Citrus sinensis* peel on type 2 diabetes mellitus (T₂DM) and Alzheimer's disease (AD).

The six identified potential inhibitors of butyrylcholinesterase and acetylcholinesterase from *Citrus sinensis* peel were retrieved from Pubchem database. The evaluation of their molecular docking score and ADME (absorption, distribution, metabolism, and excretion) – toxicity prediction of the six identified bioactive compounds was carried out with butyrylcholinesterase and acetylcholinesterase using different bioinformatics tools.

All the six compounds have a higher binding docking score than the standard used with rutin having the highest score. However, only quercetin, quercitrin and luteolin have the best ADME results and compete favorably with the standards and coligand used.

Therefore, this study suggests that quercetin, quercitrin, and luteolin might be a promising therapeutic agent in the management of both T₂DM and AD, even more, better than all standards used.

Keywords: *coligand, butyrylcholinesterase, acetylcholinesterase, management*

Introduction

According to Barbagallo and Dominguez (2014), type 2 diabetes mellitus (T2DM) and Alzheimer's disease (AD) are well known age-related disorders, and they are both categorized by increased occurrence and prevalence with aging. T2DM has been documented as one of the fastest emergent widespread disease at the moment affecting more than 422 million globally and commonly found in aged individuals (Ajiboye *et al.*, 2018). One of the main features of T2DM is hyperglycaemia due to impairment in insulin actions as well as signaling (Ajiboye *et al.*, 2019). This insulin resistance in various tissues (especially peripheral tissues) can also trigger hyperinsulinemia (Barbagallo and Dominguez, 2014). Mattson (2004) documented that AD is the furthestmost frequent neurodegenerative disorder, and its incidence rises with age. AD is characterized by continuing memory loss, cognitive dysfunctions, behavioral instability, amongst others, affecting more than 33.9 million individuals globally (Ayaz *et al.*, 2017).

Studies have reported the role of insulin and insulin resistance as a probable relative between T2DM and AD (Barbagallo and Dominguez, 2014). Although, the molecular mechanisms fundamental to are still mysterious, as well as how central and peripheral insulin signaling function in AD (Biessels and Despa, 2018). Instabilities in brain insulin signaling mechanisms could add to the molecular, biochemical, as well as histopathological lesions in AD in patients. Also, persistent hyperglycaemia might serve as a risk factor for cognitive, dementia abnormalities etc.

Hence, conventional drugs in managing T2DM patients may also be useful for AD patients *vis a vis*. But unfortunately these drugs are characterized with series of side effects, non-affordability by majority of low income earners and unavailability in the rural communities. This tips the scientists to look for natural compounds from plant origin that will be more effective in managing both T2DM and AD.

In lieu of this, an example of such plant is *Citrus sinensis* (sweet orange), is a fruit, evergreen tree of about 8 to 15 ft, and belong to a family of *Rutaceae* (Omoba *et al.*, 2015). Ehler (2011) reported that orange is commercially grown globally in tropical, semi-tropical as well as warm temperate regions. In

addition, orange (contains peel, pulp, seeds, and juice) is used globally by eaten its fresh after peeling as well as used for juice (Topuz *et al.*, 2005). The peel and seeds of orange are neglected by-products which could be used as functional ingredients in functional foods production because they are endowed with dietary fiber and bioactive compounds (Marin *et al.*, 2002). The orange peel has been reported to be a rich source of phenolic and flavonoid compounds (Omoba *et al.*, 2015). Therefore, the present study is aimed at assessing the drugability potential (using *in silico* approach) of bioactive compounds from orange peel.

Methods

Protein Preparation

In carried out molecular docking analysis, at first, retrieval of the three-dimensional crystal structure of the n-terminal subunit of the crystal structure of recombinant human acetylcholinesterase in complex with donepezil (PDB ID: 4EY7) (Cheung *et al.*, 2012) and human butyrylcholinesterase in complex with decamethonium (PDB ID: 6EP4) (Rosenberry *et al.*, 2017) in PDB format from the protein data bank. Protein Preparation Wizard of Schrödinger-Maestro v11.5.011 was used for the preparation and refinement of the retrieved target proteins. Charges and bond orders were assigned and water molecules were deleted. Hydrogens were added to the heavy atoms. Energy minimization was done by using OPLS3 force field by fixing the heavy atom RMSD of 0.30Å (Shivakumar *et al.*, 2010). Amino acids were optimized by using neutral pH.

Ligand Preparation

From the Pubchem database, the 2D structure of all the compounds from almond seed was downloaded. Ligand preparation was done to create three-dimensional geometries and to assign proper bond orders (Sastry *et al.*, 2013). Three-dimensional geometries were generated by using Ligprep2.5 in Schrödinger Suite 2018 with an OPLS3 force field. For the generation of ionization states, we used Epik4.3 in Schrödinger Suite at pH 7.0 ± 2.0 (Wizard, 2018). A maximum of 32 possible stereoisomers per ligand were obtained.

Receptor grid generation

The co-crystallized ligand for each target was used as a guide to generate a grid around the active site

that's where receptor grids were calculated for the prepared protein. For Glide docking, grids were generated by using OLPS3 force field by keeping the van der Waals scaling factor of 1.0 and charge cutoff value of 0.25. A box was generated to each direction with 60 Å × 60 Å × 60 Å for docking experiments

Extra Precision (XP) ligand docking

XP ligand docking was carried out as reported by Friesner *et al.* (2006). This docking was performed in Glide of Schrödinger-Maestro v11.5. The final result of docking can be found as a glide score by energy minimization. For docking, the van der Waals scaling factor was set to 0.85 and 0.15 for ligand compounds.

Results and Discussion

Molecular Docking analysis

Butyrylcholinesterase (BChE) and acetylcholinesterase (AChE) related proteins were found to be common to both Alzheimer disease and diabetes mellitus; they may play an etiological role via influencing insulin resistance and lipid metabolism (Sridhar *et al.*, 2006). BChE in addition to a role in co-regulating acetylcholine (ACh) levels and cholinergic neurotransmission, has noncholinergic functions related to differentiation, proliferation, and apoptosis (Darvesh *et al.*, 2003). The docking study of the compounds (as indicated in Figure 1) from *Citrus sinensis* peel revealed that the compounds may inhibit the action of human acetylcholinesterase and human butyrylcholinesterase to explore its anti-diabetic potentials via amelioration of diabetes mellitus-mediated cognitive dysfunction (Biessels and Despa, 2018). The 2 dimensional (2D) structure of all the compounds under the study is shown in Figure 2. Docking simulation of *Citrus sinensis* peel compounds to the crystal structure of recombinant human acetylcholinesterase in complex with donepezil shows the binding affinity (docking score) of coligand, metformin, rutin, quercetin, quercitrin, catechin, luteolin, epicatechin with -12.768, -4.519, -13.876, -11.558, -12.157, -10.287, -11.969, -11.057 kcal/mol respectively as shown in Table 1.

On the basis of the selection of the lead compounds, ADME toxicity parameters were used to fish-out the best compounds from the compounds under the study which knocked rutin with the highest binding score -13.876 kcal/mol off the table on human acetylcholinesterase. To further crack the anti-T2DM

and anti-AD efficacies and of *Citrus sinensis* peel, we explore the active site analysis of compounds selected versus the co-crystallized compounds and metformin/glucofage (preferred first-line oral blood-glucose-lowering agent to manage type 2 diabetes) (Clifford, 2017). The coligand (donepezil) was able to interact with the key amino acid residue for inhibition of human acetylcholinesterase. The aromatic group at the two ends of coligand (donepezil) are in the same positions: the benzyl ring stacks against Trp86 in the active site, while the indanone ring stacks against Trp286 in the peripheral anionic site. The narrower gorge in rhAChE, created by different positions of Trp337 and Trp341, results in a conformation where piperidine ring packs against the hydrophobic portions of the side chains of Trp337, Phe338 with pi-cation (Cheung *et al.*, 2017) as shown in Figure 3. All these amino acid residues were found within 4Å of metformin within the human acetylcholinesterase but showed no bond communication except for Glu202 with two (2) hydrogen bond aided by salt bridge shown Figure 4. Quercetin from *Citrus sinensis* peel was able to interact with the reported resident amino acid for human acetylcholinesterase inhibition. The benzyl ring of quercetin double pi-stack against Phe338, but exhibit single pi-stacking with His447 with stability with hydrogen bond with Gly122 and the phenoxyl rig accept hydrogen bond from Phe295 as shown in Figure 5. Quercitrin was able to pi-stack against Trp286 with double pi-pi stacking bond and stability with Phe295, Ser293, Gln292 and Tyr72 by hydrogen bond network. Also investigating the anti-T2DM and anti-AD potentials of *Citrus sinensis* peel on human butyrylcholinesterase (acetylcholinesterase counterpart) in the etiologies of these diseases. The compounds were docked into the active site of the target protein. Rutin with the highest docking score (-15.424 kcal/mol) was knocked off by ADME toxicity parameter, on this basis, the selected compounds were quercetin, quercitrin, and luteolin with -11.278, -10.204, -9.248, -9.186 and -8.188 kcal/mol respectively as shown in Table 1. According to Li *et al* (2019), the molecular docking is an attractive tool in drug discovery as well as in molecular modeling presentations. The dependability of this docking depends on the accuracy of the embraced scoring function, which also guide and determine the ligand poses when a series of promising poses of ligands are

produced. This scoring function indeed can be used in determining the binding mode and site of a ligand, predict binding affinity and identify a possible drug leads for a given protein target (Huang *et al.*, 2010). The analyses of the binding pose of the docked compounds versus the co-crystallized ligand (Decamethonium) and metformin. Figure 7 displayed the inhibitory efficacy of human butyrylcholinesterase via interaction with the reported resident amino acids that drive butyrylcholinesterase inhibition. Decamethonium spans the gorge of hBChE from the gorge entrance to the choline-binding pocket (Figure 7), where the deeper quaternary group interacts with Trp82 and Glu197. It is noteworthy that this Glu197, which is conserved among cholinesterases, has an unusually high pKa and can be protonated at neutral pH (Driant *et al.*, 2017). It follows that the interaction of Glu197 with the quaternary ammonium moiety of decamethonium is not necessarily ionic but could involve a hydrogen bond (Berg *et al.*, 2016). Ala328, forms a 90° bend and proceeds towards the gorge entrance where the second quaternary group is at the right distance to interact with Tyr332 at the P-site thus support that Tyr332 is a key element of the P-site of hBChE (Rosenberry *et al.*, 2017).

The same set of resident amino acids found around the coligand is seen around the standard drug (metformin) for the treatment of diabetes mellitus, display hydrogen bond and salt-bridge with Asp70 as shown in Figure 8. Luteolin pack pi-pi stacking against Trp82 and its phenol ring is stabilized within butyrylcholinesterase active site with two (2) hydrogen bond donor with Ala328 which proceeds towards the gorge entrance where the second quaternary group is at the right distance to interact with Tyr332 at the P-site as seen crystallized ligand and the other end phenol ring with Thr120 which is as shown in Figure 9. Quercetin also interacts with the Trp82 with double pi-pi stacking and stabilized with hydrogen bond donor to Ala328, Thr120, and Gly155 shown in Figure 10. Quercitrin also interacts with one of the key resident amino acid residues with hydrogen bond with Trp82 and His438 as shown in Figures 6 and 11.

ADME analysis

The ADME properties of targets cocrystallized ligand, standard drug (metformin) and compounds under the study were evaluated to elucidate their

pharmacokinetic properties. Table 2 illustrates ADME properties of these compounds. These properties represent the bioavailability, distribution, cell permeability, excretion and absorption quality of the compounds; also ADME pronounces the disposition and fate of pharmaceutical compounds inside an organism, particularly in the human body. The main cause of the disappointment in the drug development phase is poor pharmacokinetics as well as toxicity rather than poor efficiency of the candidate compound (Shin *et al.*, 2017). From the results of ADME analysis, it was observed that the predicted blood or brain barrier permeability of the cocrystallized ligand of human acetylcholinesterase (donepezil) and human butyrylcholinesterase (decamethonium) standard compound metformin is still within the acceptable range except for donepezil which lesser than the acceptable ranges and this parameter is very important for a drug to pass through those barriers. All the compounds showed acceptable range QPlogBB value of -3.0-1.2, except in rutin (-5.015), this is support anti-T2DM and anti-AD of the selected compounds. The number of hydrogen bonds donor and acceptor are in the value of acceptable range and solvent-accessible surface area (SASA) also showed acceptable value except for the donepezil, rutin, and decamethonium. The predicted IC₅₀ value for blocking HERG K⁺ channel showed acceptable range except for both metformin and rutin that showed lesser values with -2.938 and -6.119 respectively and the acceptable range below-5. The predicted octanol or water partition coefficient for all compounds and the cocrystallized ligands were also analyzed. All compounds were found within the acceptable range except for decamethonium with higher value (9.802) and the acceptable range is -2.0 to 6.5. The human oral absorption rate was also greater for all compounds and cocrystallized ligand (50%) except quercitrin and rutin lesser value (<25%) according to the findings of this study. In the case of cell permeability, all compounds showed lower value and decamethonium is above the normal value and this is a key parameter for a drug to pass through the cell to be active. Skin permeability all compounds, metformin, and cocrystallized ligands are close to the acceptable range -8.0 to -10.0. The obtained results revealed that quercetin, quercitrin and luteolin are all druggable targets for the management of both

T2DM and AD, this supports the antioxidant nature of these compounds as reported by Omoba *et al.* (2015).

. Conclusion

Docking is one of the most crucial computational tools used in predicting the activity of the potential drug. It can be deduced from this study that although rutin has the highest molecular docking score but it has bad ADMET results. Therefore, only quercetin, quercitrin and luteolin might be a promising therapeutic agent in the management of both T2DM and AD from the orange peel.

Conflicts of interest

The author declares no conflict of interest

References

Ayaz, M., Junaid, M., Ullah, F., Subhan, F., Sadiq, A., Ali, G., Ahmad, S. (2017). Anti-Alzheimer's studies on β -sitosterol isolated from *Polygonum hydropiper* L. *Frontiers in pharmacology*, 8, 697. <https://doi.org/10.3389/fphar.2017.00697>.

Barbagallo, M. and Dominguez, L. J. (2014). Type 2 diabetes mellitus and Alzheimer's disease. *World J Diabetes*. 5(6): 889-893

Berg, L., Mishra, B.K., Andersson, C.D., Ekstrom, F. and Linusson, A. (2016). The Nature of Activated Non-Classical Hydrogen Bonds: A Case Study on Acetylcholinesterase-Ligand Complexes. *Chemistry*, 22: 2672-2681.

Biessels, G. J., and Despa, F. (2018). Cognitive decline and dementia in diabetes mellitus: mechanisms and clinical implications. *Nat. Rev. Endocrinol.* 14: 591-604. doi: 10.1038/s41574-018-0048-7

Biessels, G. J., and Despa, F. (2018). Cognitive decline and dementia in diabetes mellitus: mechanisms and clinical implications. *Nature Reviews Endocrinology*, 14(10), 591-604.

Cheung, J., Rudolph, M. J., Burshteyn, F., Cassidy, M. S., Gary, E. N., Love, J. and Height, J. J. (2012). Structures of human acetylcholinesterase in complex with pharmacologically important ligands. *Journal of Medicinal Chemistry*, 55(22), 10282-10286.

Darvesh, S., Hopkins, D.A. and Geula, C. (2003). Neurobiology of butyrylcholinesterase. *Nat Rev Neurosci* 4:131-138.

Driant, T., Nachon, F., Ollivier, C., Renard, P.Y. and Derat, E. (2017). On the Influence of the Protonation States of Active Site Residues on AChE Reactivation: A QM/MM Approach. *ChemBioChem*. 18:666-675.

Ehler, S.A. (2011). Citrus and its benefits. *J. Bot.* 5: 201-207

Friesner, R.A., Murphy, R.B., Repasky, M.P., Frye, L.L., Greenwood, J.R., Halgren, T.A., Sanschagrin, P.C. and Mainz, D. T. (2006). Extra precision glide: Docking and scoring incorporating a model of hydrophobic enclosure for protein-ligand complexes. *Journal of Medicinal Chemistry*. 49(21): 6177-6196.

Huang, S.Y., Grinter, S.Z. and Zou, X. (2010) Scoring functions and their evaluation methods for protein-ligand docking: recent advances and future directions. *Phys Chem Chem Phys* PCCP 12(40):12899-12908.

Kamal, M. A., Tan, Y., Seale, J. P., and Qu, X. (2009). Targeting BuChE-inflammatory pathway by SK0506 to manage type 2 diabetes and Alzheimer disease. *Neurochemical research*, 34(12), 2163.

Li, J., Fu, A. and Zhang, L. (2019). An Overview of Scoring Functions Used for Protein-Ligand Interactions in Molecular Docking. *Interdisciplinary Sciences: Computational Life Sciences*, 11: 320-328

Marin, F.R., Martinez, M.T., Uribealago, S.C. and Frutos, M.J. (2002). Changes in nutraceutical composition of lemon juices according to different industrial extraction systems. *Food Chem*. 78, 319-324

Mattson, M.P. (2004). Pathways towards and away from Alzheimer's disease. *Nature*. 430: 631-639. DOI: 10.1038/nature02621.

Omoba, O.S., Obafaye, R.O., Salawu, S.O., Boligon, A.A and Athayde, M.L. (2015). HPLC-DAD Phenolic Characterization and Antioxidant Activities of Ripe and Unripe Sweet Orange Peels. *Antioxidants*. 4: 498-512; doi:10.3390/antiox4030498

Rosenberry, T. L., Brazzolotto, X., Macdonald, I. R., Wandhammer, M., Trovaslet-Leroy, M., Darvesh, S. and Nachon, F. (2017). Comparison of the binding of reversible inhibitors to human butyrylcholinesterase and acetylcholinesterase: A crystallographic, kinetic and calorimetric study. *Molecules*, 22(12), 2098.

Sastry, G.M., Adzhigirey, M., Day, T., Annabhimoju, R. and Sherman, W. (2013). Protein and ligand preparation: parameters, protocols, and influence on virtual screening enrichments. *Journal of Computer-aided Molecular Design*, 27(3): p. 221-234.

Shin, H.K., Young-Mook, K, and No, K.T. (2017). Predicting ADME Properties of Chemicals. J. Leszczynski et al. (eds.), DOI 10.1007/978-94-007-6169-8_59-1

Shivakumar, D., Williams, J., Wu, Y., Damm, W., Shelley, J. and Sherman, W. (2010). Prediction of absolute solvation free energies using molecular dynamics free energy perturbation and the OPLS force field. *Journal of Chemical Theory and Computation*, 2010. 6(5): 1509-1519.

Sridhar GR, Thota H, Allam AR, Babu CS, Prasad AS, Divakar CH (2006) Alzheimer's disease and type 2 diabetes mellitus: the cholinesterase connection? *Lipids Health Dis.* 5:28.

Topuz, A., Topakci, M., Canakci, M., Akinci, I., and Ozdemir, F. (2005). Physical and nutritional properties of four orange varieties. *J. Food Eng.* 66: 519–523

Wizard, P.P. (2018). Epik version 4.3, Impact version 7.8, Prime version 5.1. New York, NY: Schrödinger, LLC

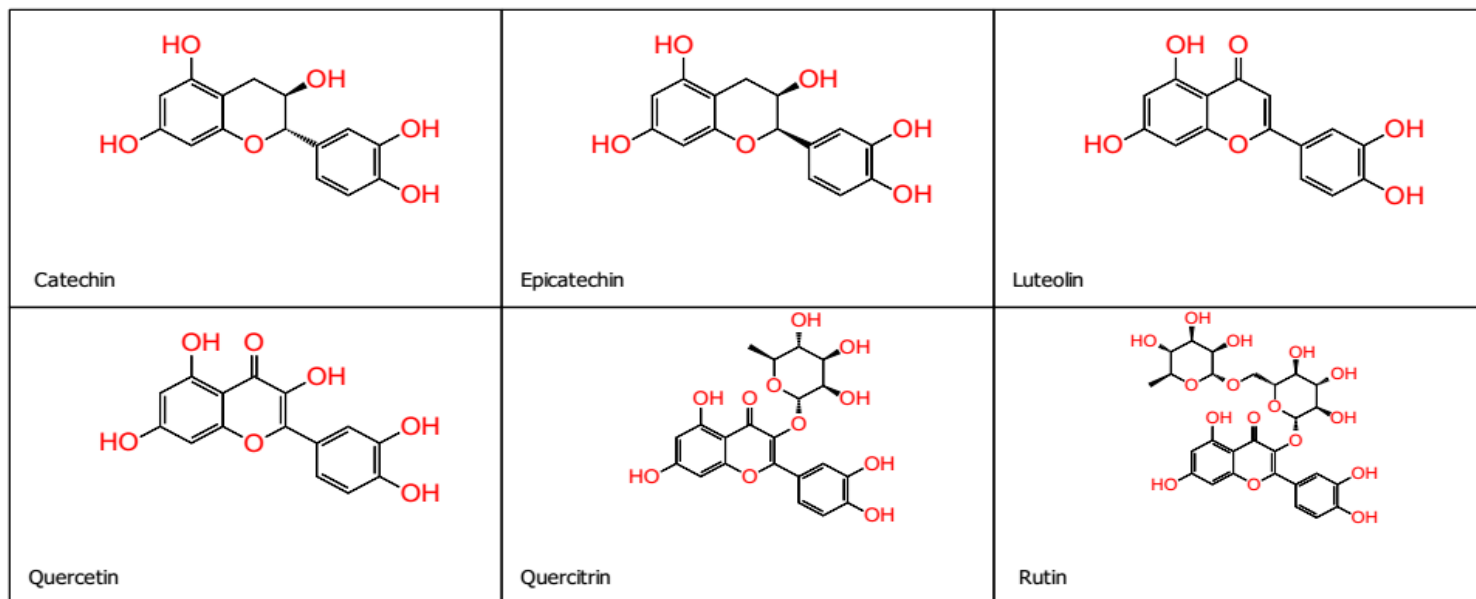
Figure 1: Two dimensional (2D) structures of compounds from *Citrus sinensis* peel

Figure 2: Three dimensional (3D) structures of the target proteins. **(a)** Crystal structure of recombinant human acetylcholinesterase in complex with donepezil (surface binding site). **(b)** Human butyrylcholinesterase in Complex with decamethonium (surface binding site)

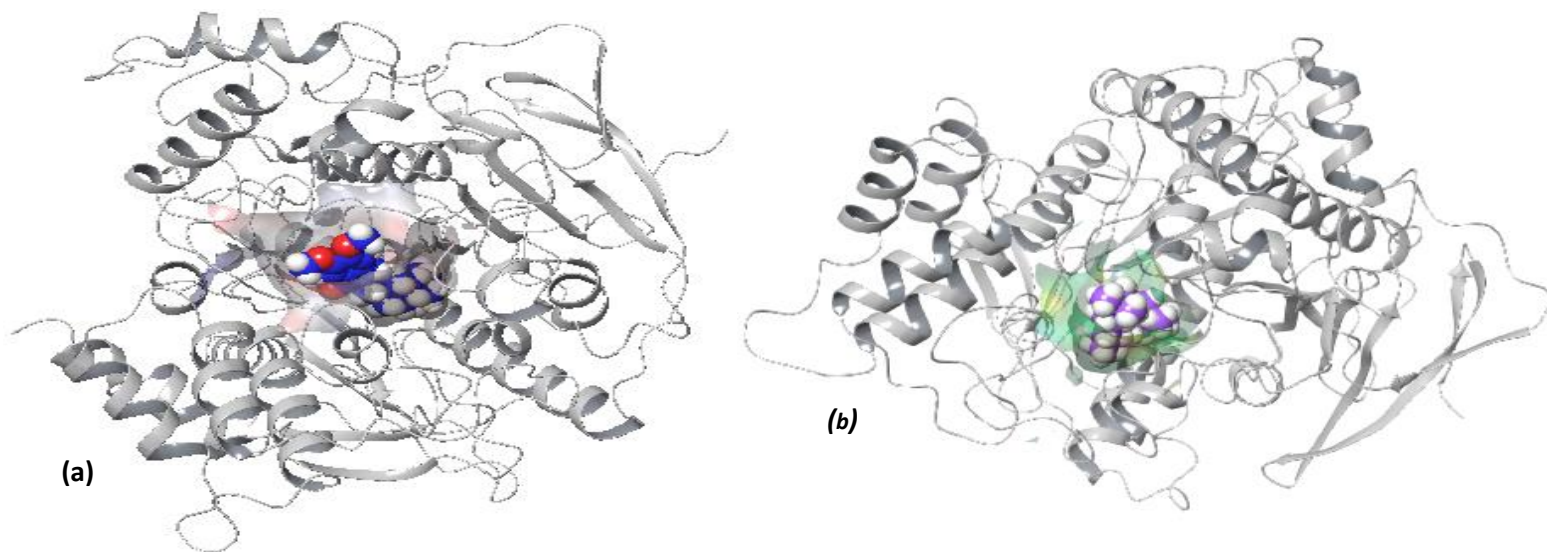



















Figure 1: Structural representation of Molecular docking analysis of Crystal structure of recombinant human acetylcholinesterase in complex with donepezil. Donepezil made interactions with the residues of the active site. (a) The image explains the two dimensional binding pattern of Donepezil with human acetylcholinesterase. (b) The image gives three dimensional overview of the interaction of Donepezil with human acetylcholinesterase

- | | | | |
|--|--|--|--|
|  Charged (negative) |  Polar |  Distance |  Salt bridge |
|  Charged (positive) |  Unspecified residue |  H-bond |  Solvent exposure |
|  Glycine |  Water |  Metal coordination | |
|  Hydrophobic |  Hydration site |  Pi-Pi stacking | |
|  Metal |  Hydration site (displaced) |  Pi-cation | |

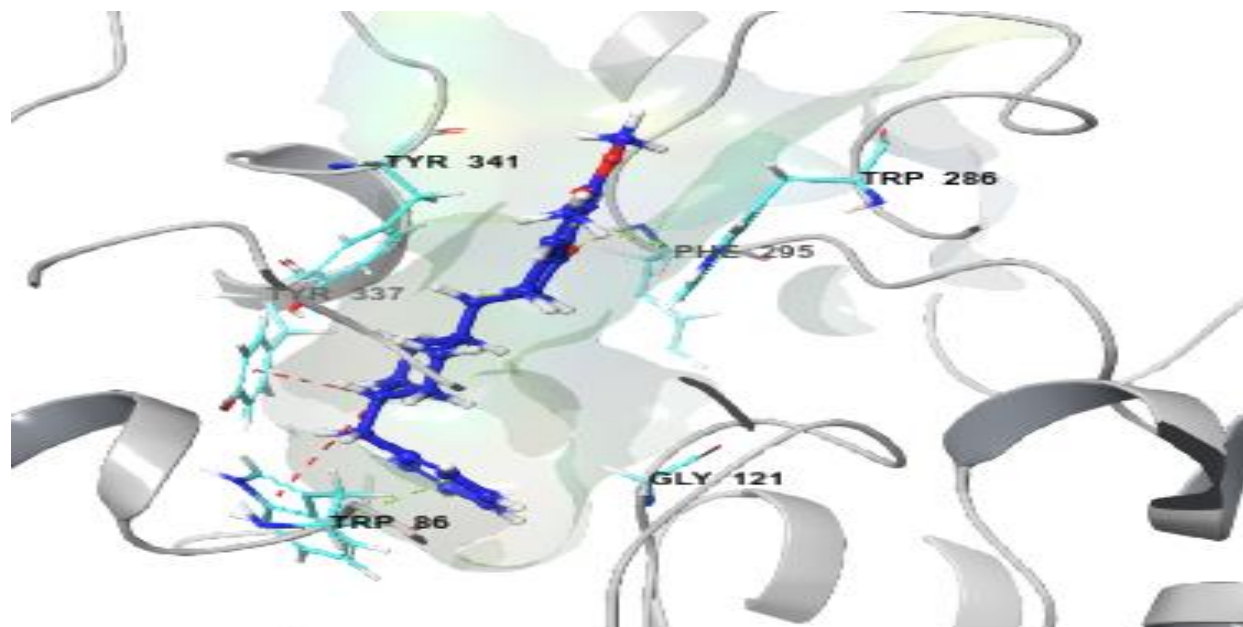
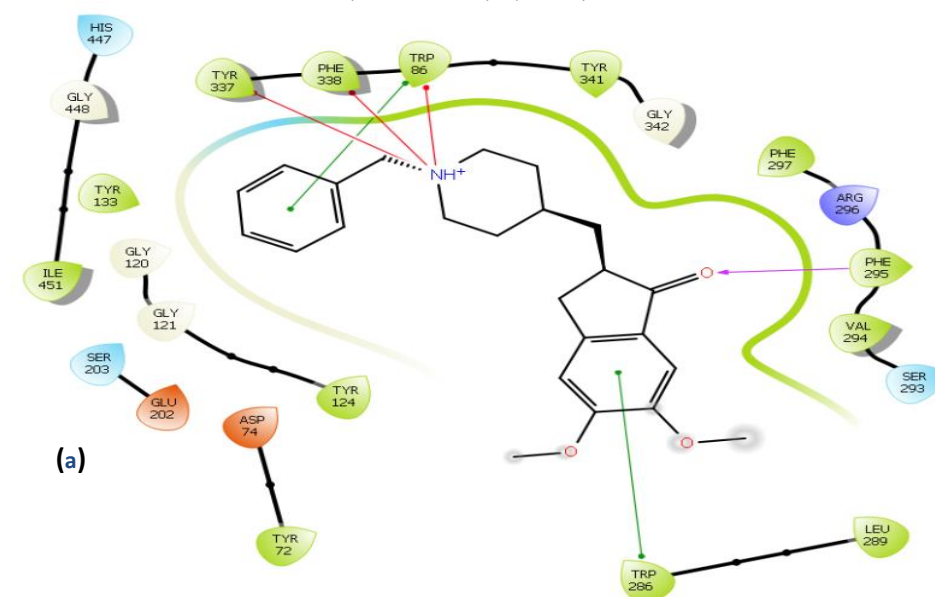


Figure 4: Structural representation of Molecular docking analysis of metformin within the crystal structure of recombinant human acetylcholinesterase in complex with donepezil. Metformin made interactions with the residues of the active site. (a) The image explains the two dimensional binding pattern of metformin with human acetylcholinesterase. (b) The image gives three dimensional overview of the interaction of metformin with human acetylcholinesterase

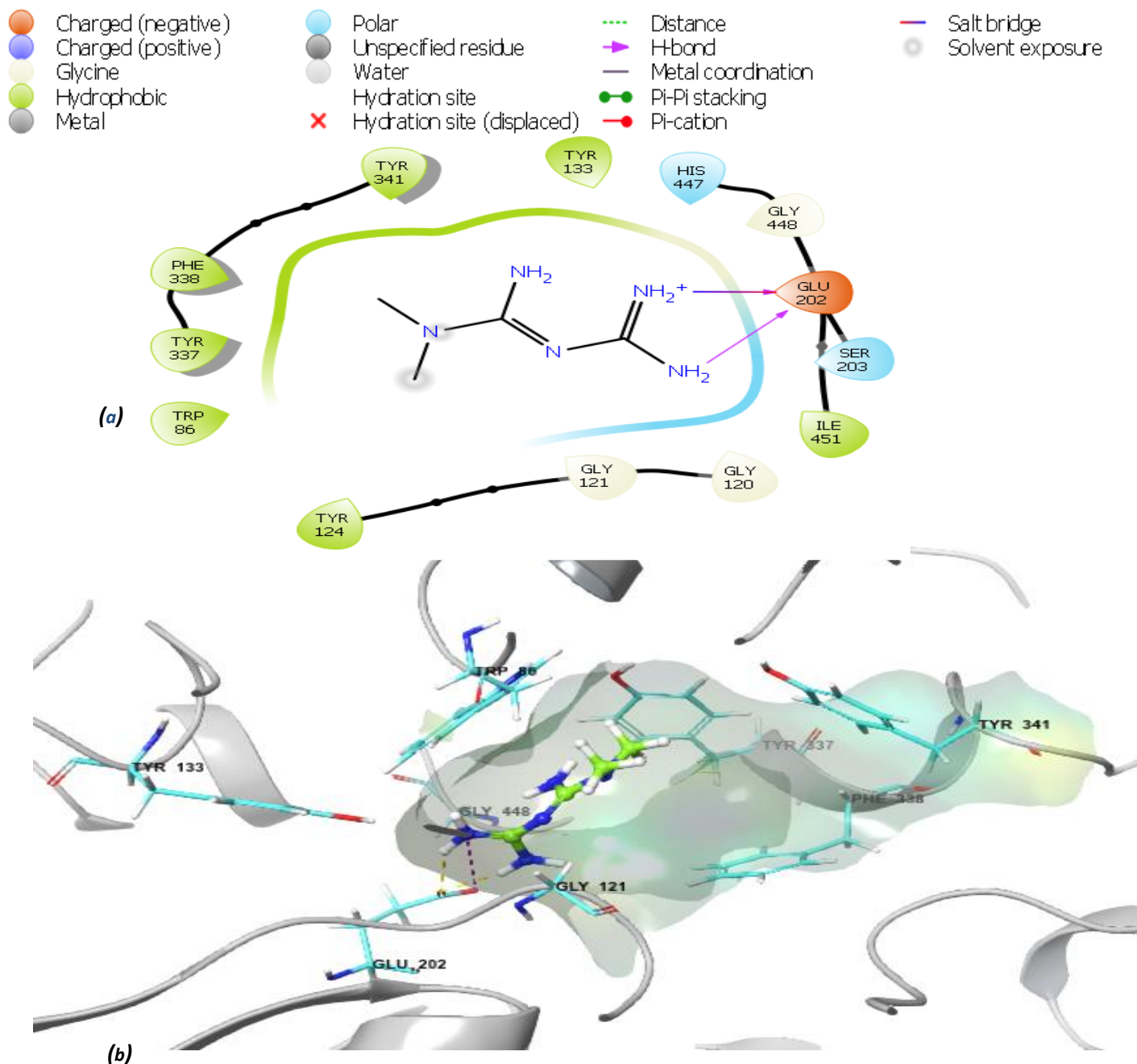





Figure 5: Structural representation of Molecular docking analysis of quercetin within the crystal structure of recombinant human acetylcholinesterase in complex with donepezil. Quercetin made interactions with the residues of the active site. (a) The image explains the two dimensional binding pattern of quercetin with human acetylcholinesterase. (b) The image gives three dimensional overview of the interaction of quercetin with human acetylcholinesterase

- | | | | |
|--|--|--|--|
|  Charged (negative) |  Polar |  Distance |  Salt bridge |
|  Charged (positive) |  Unspecified residue |  H-bond |  Solvent exposure |
|  Glycine |  Water |  Metal coordination | |
|  Hydrophobic |  Hydration site |  Pi-Pi stacking | |
|  Metal |  Hydration site (displaced) |  Pi-cation | |

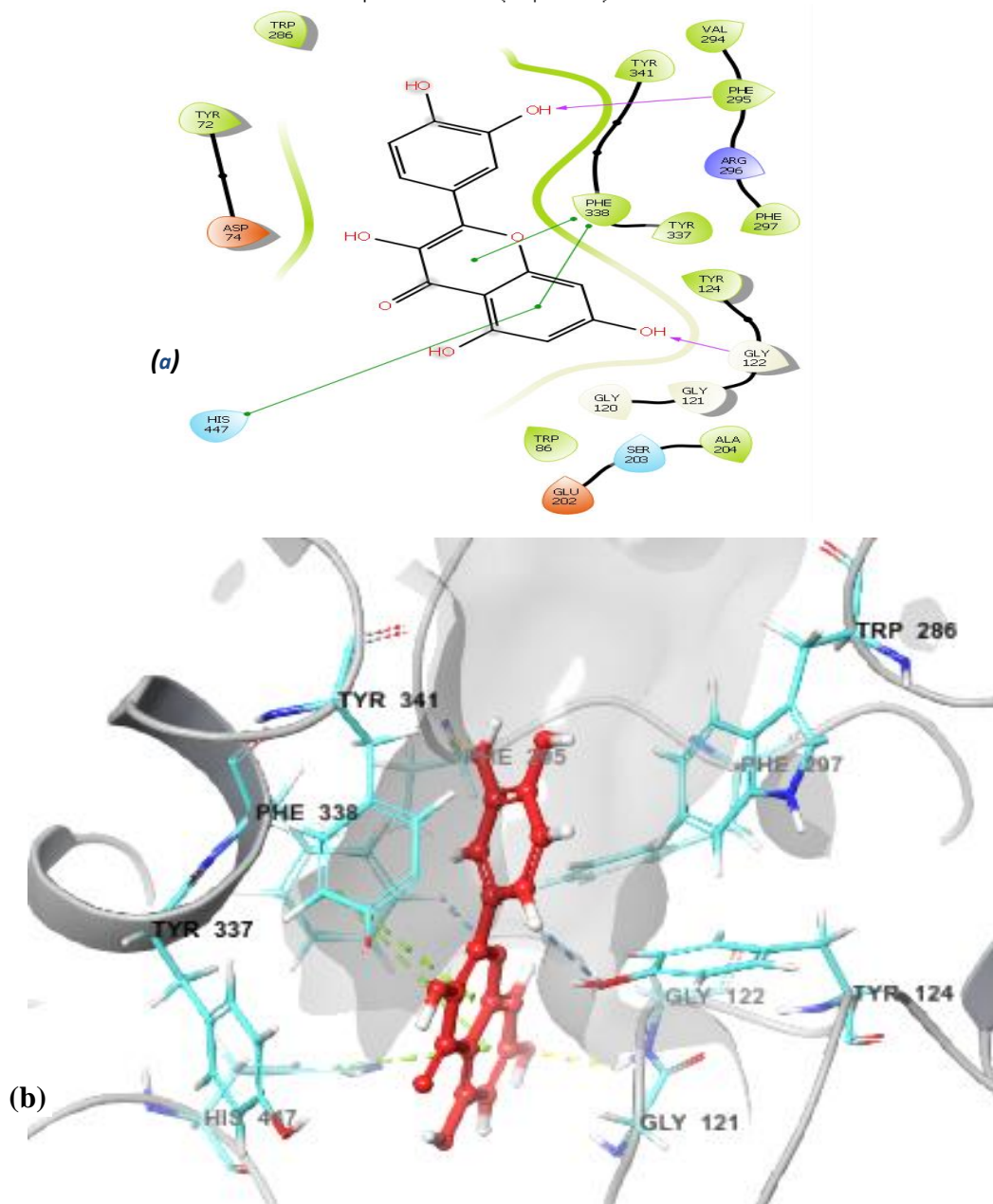

















Figure 6: Structural representation of Molecular docking analysis of quercitrin within the crystal structure of recombinant human acetylcholinesterase in complex with donepezil. Quercitrin made interactions with the residues of the active site. **(a)** The image explains the two dimensional binding pattern of quercitrin with human acetylcholinesterase. **(b)** The image gives three dimensional overview of the interaction of quercitrin with human acetylcholinesterase.

- | | | | |
|--|--|--|--|
|  Charged (negative) |  Polar |  Distance |  Salt bridge |
|  Charged (positive) |  Unspecified residue |  H-bond |  Solvent exposure |
|  Glycine |  Water |  Metal coordination | |
|  Hydrophobic |  Hydration site |  Pi-Pi stacking | |
|  Metal |  Hydration site (displaced) |  Pi-cation | |

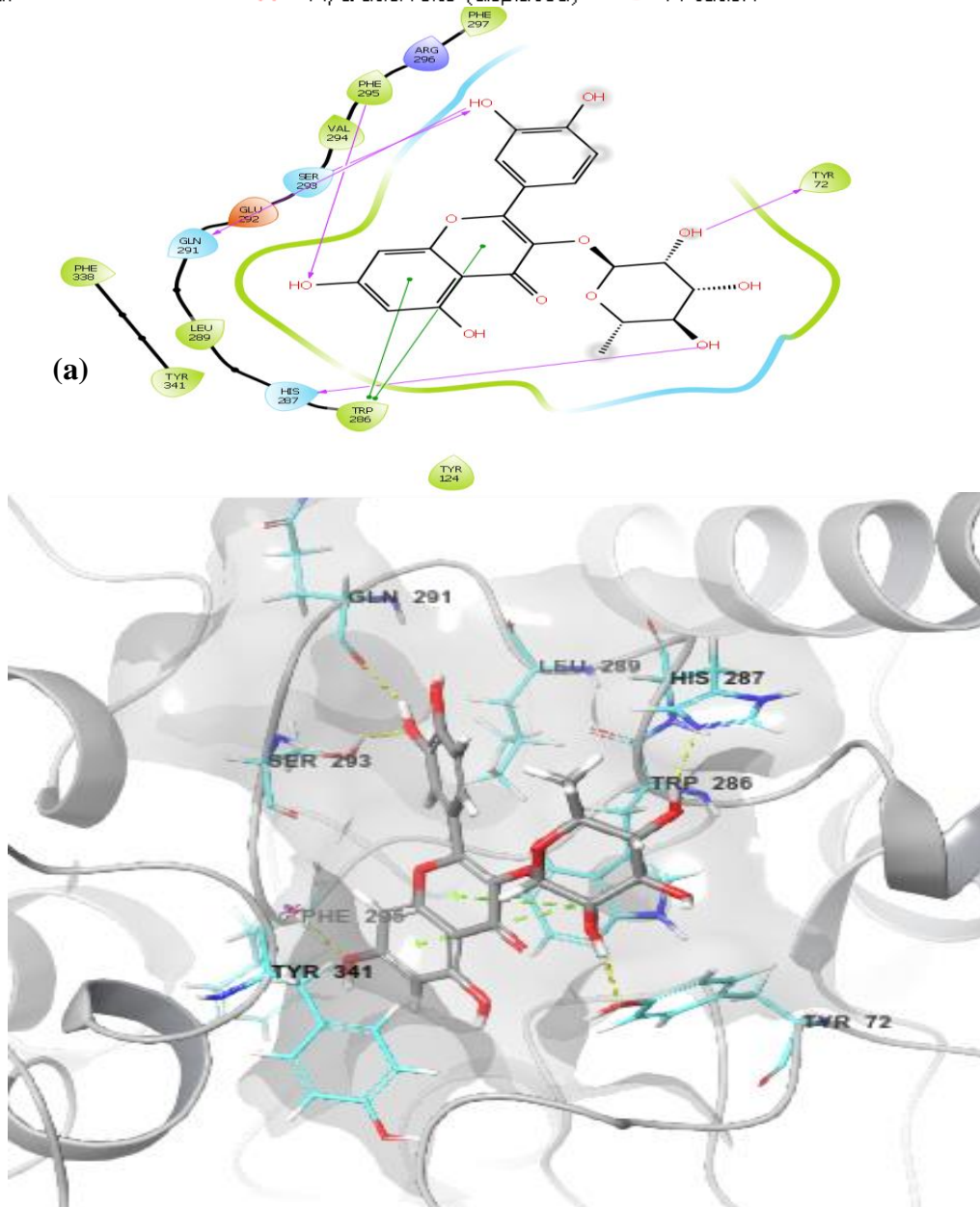







Figure 8: Structural representation of Molecular docking analysis of metformin within the crystal structure of human butyrylcholinesterase in complex with decamethonium. Metformin made interactions with the residues of the active site. (a) The image explains the two dimensional binding pattern of metformin with human butyrylcholinesterase. (b) The image gives three dimensional overview of the interaction.

- | | | | |
|--|--|--|--|
|  Charged (negative) |  Polar |  Distance |  Salt bridge |
|  Charged (positive) |  Unspecified residue |  H-bond |  Solvent exposure |
|  Glycine |  Water |  Metal coordination | |
|  Hydrophobic |  Hydration site (displaced) |  Pi-Pi stacking | |
|  Metal | |  Pi-cation | |

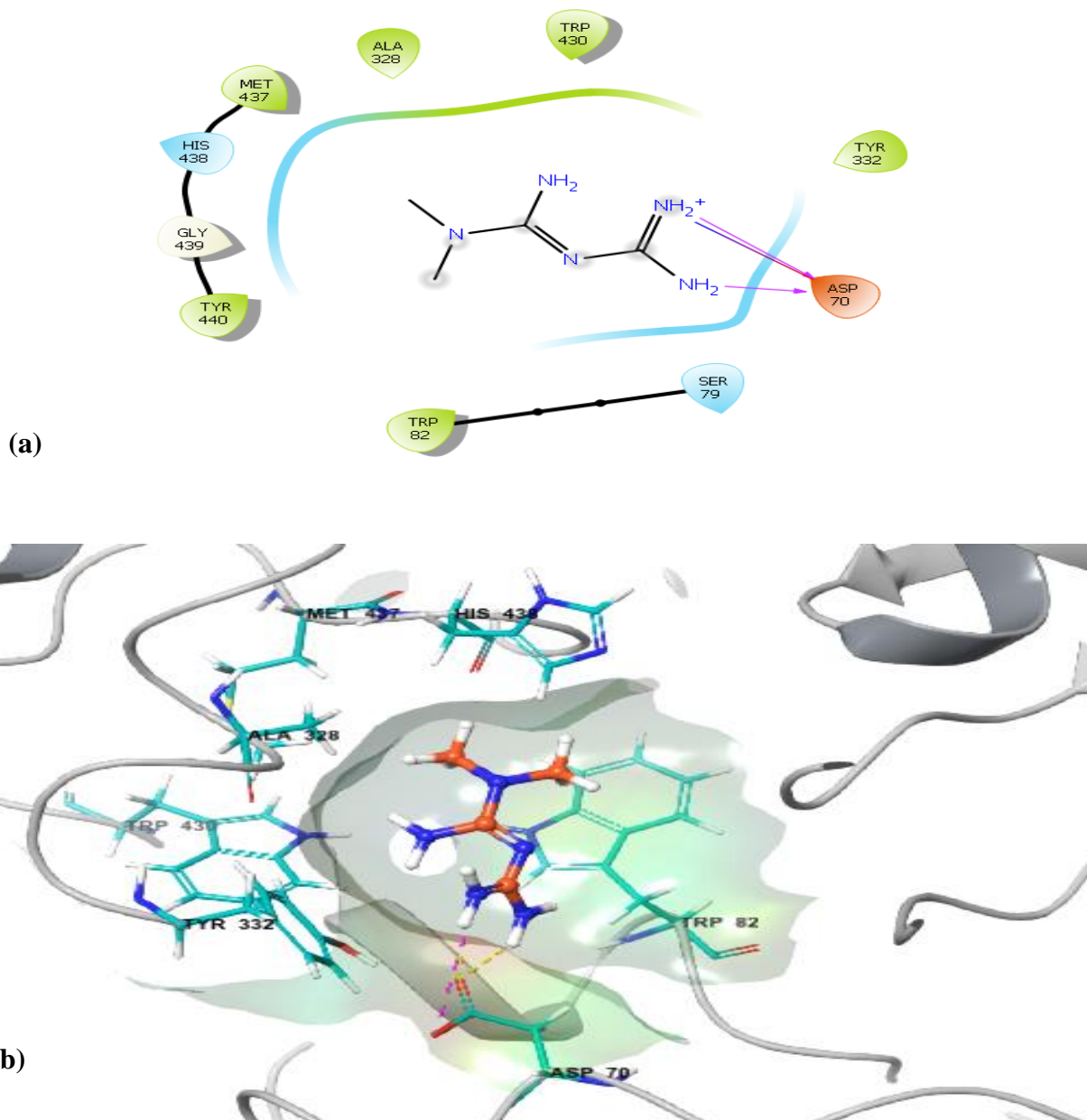


Figure 9: Structural representation of Molecular docking analysis of luteolin within the crystal structure of human butyrylcholinesterase in complex with decamethonium. Luteolin made interactions with the residues of the active site. (a) The image explains the two dimensional binding pattern of luteolin with human butyrylcholinesterase. (b) The image gives three dimensional overview of the interaction of luteolin with human butyrylcholinesterase.

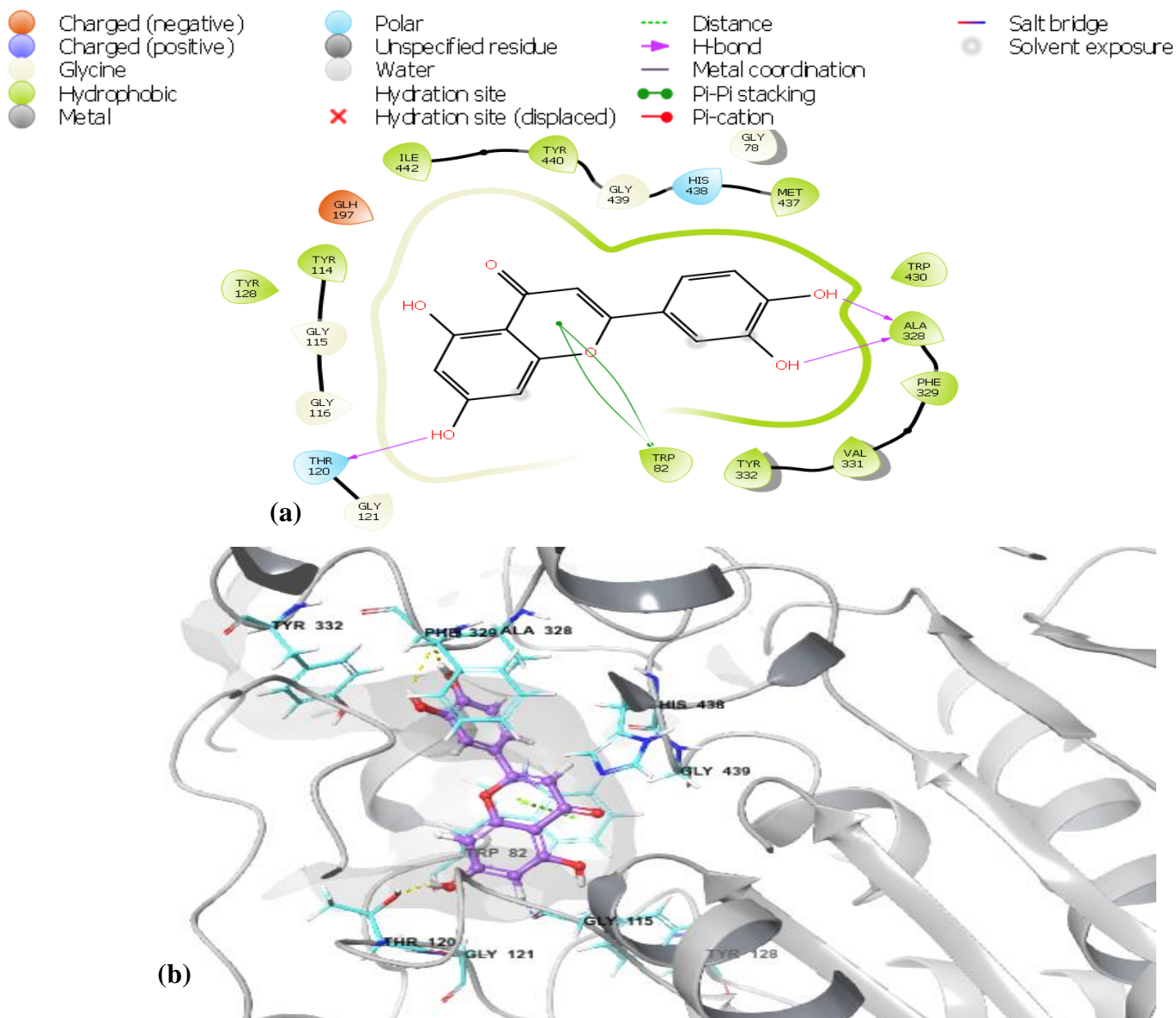


Figure 10: Structural representation of Molecular docking analysis of quercetin within the crystal structure of human butyrylcholinesterase in complex with decamethonium. Quercetin made interactions with the residues of the active site. (a) The image explains the two dimensional binding pattern of quercetin with human butyrylcholinesterase. (b) The image gives three dimensional overview of the interaction of quercetin with human butyrylcholinesterase

- | | | | |
|--|--|--|--|
|  Charged (negative) |  Polar |  Distance |  Salt bridge |
|  Charged (positive) |  Unspecified residue |  H-bond |  Solvent exposure |
|  Glycine |  Water |  Metal coordination | |
|  Hydrophobic |  Hydration site |  Pi-Pi stacking | |
|  Metal |  Hydration site (displaced) |  Pi-cation | |

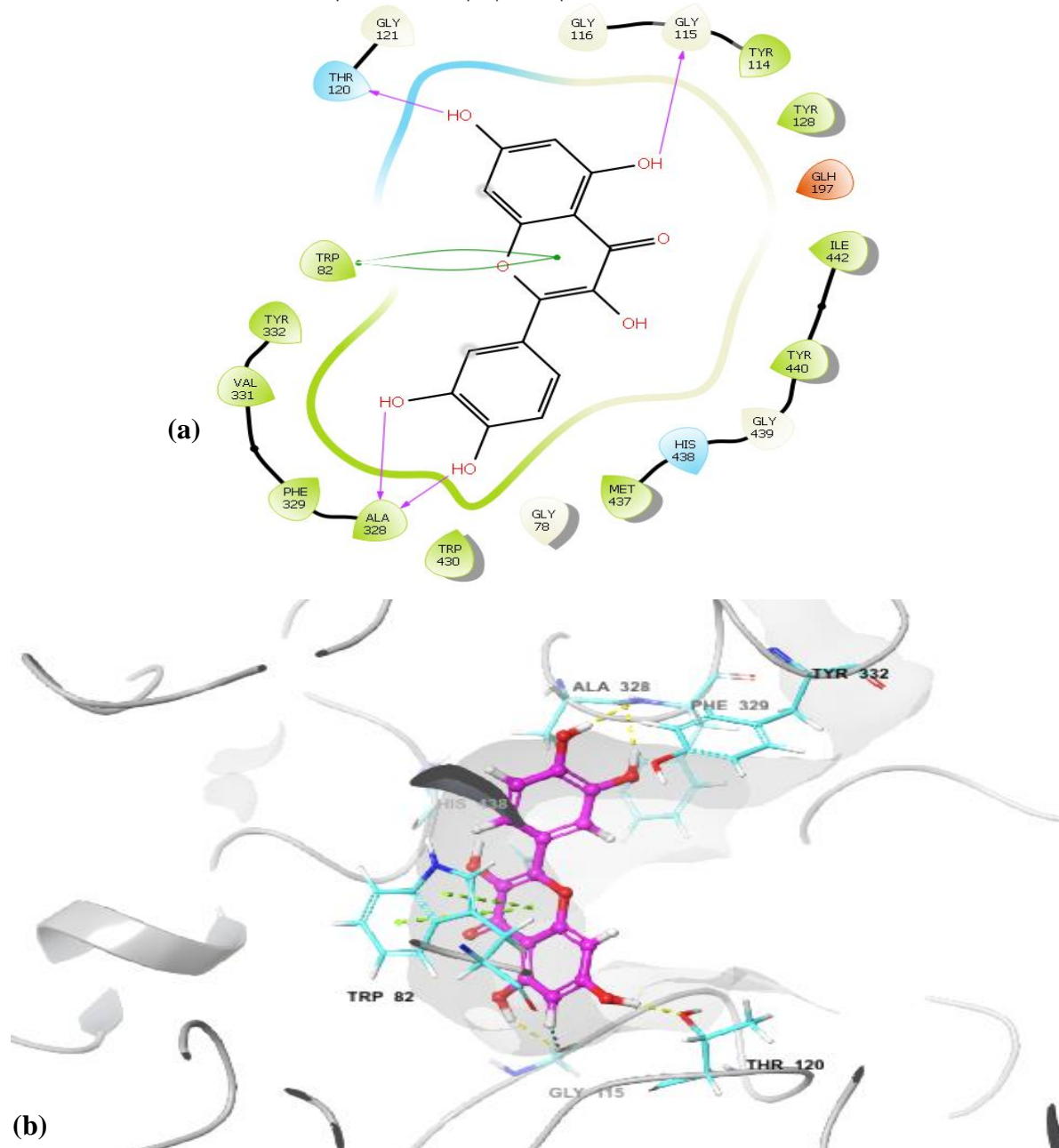



















Figure 11: Structural representation of Molecular docking analysis of quercetrin within the crystal structure of human butyrylcholinesterase in Complex with decamethonium. Quercetrin made interactions with the residues of the active site. (a) The image explains the two dimensional binding pattern of quercetrin with human butyrylcholinesterase. (b) The image gives three dimensional overview of the interaction of quercetrin with human butyrylcholinesterase

- | | | | |
|--|--|--|--|
|  Charged (negative) |  Polar |  Distance |  Salt bridge |
|  Charged (positive) |  Unspecified residue |  H-bond |  Solvent exposure |
|  Glycine |  Water |  Metal coordination | |
|  Hydrophobic |  Hydration site |  Pi-Pi stacking | |
|  Metal |  Hydration site (displaced) |  Pi-cation | |

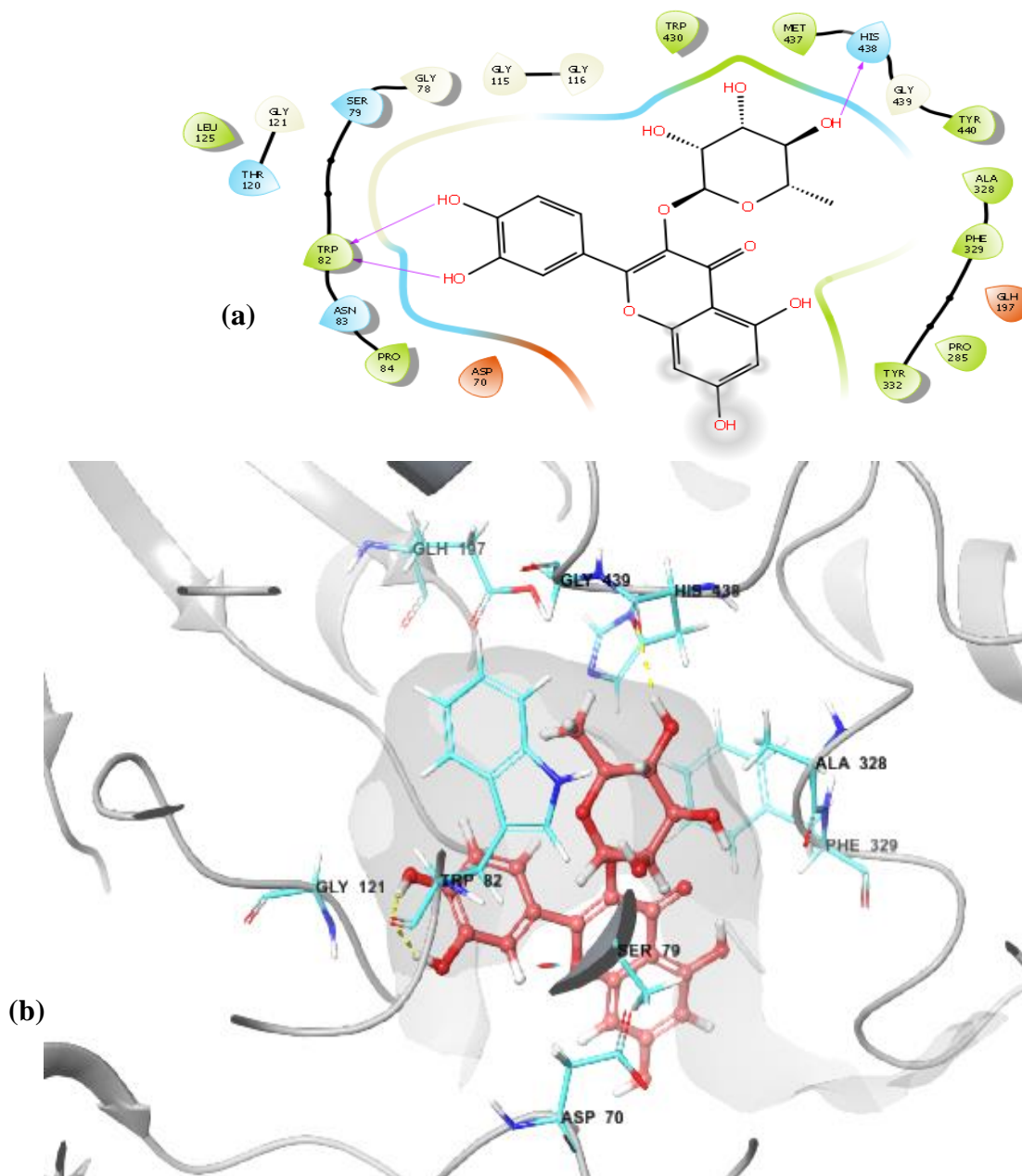


Table 1: Showing the molecular docking results (kcal/mol) of compounds with molecular targets

Compounds	Human Butyrylcholinesterase	Human Acetylcholinesterase
Coligand	-3.641	-12.768
Metformin	-3.941	-4.519
Rutin	-15.424	-13.876
Quercetin	-11.278	-11.558
Quercitrin	-10.204	-12.157
Catechin	-9.248	-10.287
Luteolin	-9.186	-11.969
Epicatechin	-8.189	-11.057

Table 2: ADME properties of compounds using Qikprop

Compounds	SASA	DonorHB	AccptHB	QPlogPo/w	QPlogS	QPlogHERG	QPlogBB	QPPMDCK	QPlogKp	%HOA
Catechin	512.552	5	5.45	0.45	-2.631	-4.778	-1.916	19.44	-4.768	59.997
Epicatechin	507.156	5	5.45	0.457	-2.554	-4.638	-1.848	21.347	-4.718	60.713
Luteolin	501.948	3	4.5	0.927	-3.069	-5.025	-1.956	15.593	-4.888	61.208
Quercetin	519.332	4	5.25	0.368	-2.91	-5.109	-2.419	6.511	-5.543	51.655
Quercitrin	654.108	6	12.05	-0.534	-2.939	-5.096	-3.118	2.33	-6.058	13.066
Rutin	851.242	9	20.55	-2.443	-2.771	-6.119	-5.015	0.266	-7.163	0
Decamethonium	648.763	0	0	9.802	-10.518	-4.555	1.491	5899.293	4.601	100
donepezil	707.126	0	5.5	4.295	-4.541	-6.587	0.057	421.195	-3.138	100
metformin	338.281	5	3.5	-0.712	-0.448	-2.983	-1.034	107.067	-6.289	65.467

Legend: Predicted blood/brain partition coefficient, QPlogBB = -3.0-1.2

Hydrogen bonds donor, HB donor = 0.0-6.0

Hydrogen bonds acceptor, HB acceptor = 2.0-20.0

Total solvent accessible surface area, SASA = 300.0-1000.0

Predicted IC₅₀ value for blockage of HERG K⁺ channels, QPlogHERG = Concern below -5

Predicted aqueous solubility, QPlogS = -6.5-0.5

Predicted octanol/water partition coefficient, QP log Po/w = -2.0-6.5

Predicted qualitative human oral Absorption,(%) = >80% is high, <25% is poor

Predicted apparent MDCK cell permeability in nm/sec, QPPMDCK= >500 is great, <25 is poor

Predicted skin permeability, QPlogKp = -8.0 to -10.0